Automatic Gain Control (AGC) as an Interference Assessment Tool

Frederic Bastide, ENAC/STNA, France
Dennis Akos, Stanford University
Christophe Macabiau, ENAC, France
Benoit Roturier, STNA, France

BIOGRAPHIES

Frederic Bastide graduated as an electronics engineers at the ENAC, the French university of civil aviation, in 2001, Toulouse. He is now a Ph.D student at the ENAC. His researches focus on the study of dual frequencies receivers for civil aviation use. Currently he is working on DME/TACAN signals impact on GNSS receivers. He also spent 6 months at the Stanford GPS Lab earlier this year as an exchange researcher.

Dennis M. Akos completed the Ph.D. degree in Electrical Engineering at Ohio University conducting his graduate research within the Avionics Engineering Center. After completing his graduation he has served as a faculty member with Luleå Technical University, Sweden and is currently a research associate with the GPS Laboratory at Stanford University. His research interests include GPS/CDMA receiver architectures, RF design, and software radios.

Christophe Macabiau graduated as an electronics engineer in 1992 from the ENAC (Ecole Nationale de l'Aviation Civile) in Toulouse, France. Since 1994, he has been working on the application of satellite navigation techniques to civil aviation. He received his Ph.D. in 1997 and has been in charge of the signal processing lab of the ENAC since 2000.

Benoit Roturier graduated as a CNS systems engineer from Ecole Nationale de l'Aviation Civile (ENAC), Toulouse in 1985 and obtained a PhD in Electronics from Institut National Polytechnique de Toulouse in 1995. He was successively in charge of Instrument Landing Systems at DGAC/STNA (Service Technique de la Navigation Aerienne), then of research activities on CNS systems at ENAC. He is now head of GNSS Navigation subdivision at STNA and is involved in the development of civil aviation applications based on GPS/ABAS, EGNOS and Galileo.

ABSTRACT

Automatic Gain Control (AGC) is a very important component in a Global Navigation Satellite System (GNSS) receiver. Such functionality is required anytime multibit quantization is implemented so as to lower quantization losses. In GNSS receivers, where the signal power is below that of the thermal noise floor, the AGC is driven by the ambient noise environment rather than the signal power. As a result, AGC can be a valuable tool for assessing the operating environment of a GNSS receiver. AGC and its functionality are investigated throughout this paper.

Behavior of this system, both in the nominal thermal noise environment as well as when the AGC circuit will be subjected to various types of interference, are examined. Its usefulness as an interference detection and estimation tool is highlighted through several tests using simulated and real signals. Moreover, the frequency assignment of the proposed GPS L5 signal is expected to face a significant interference environment as a result of other aviation systems operate in or near band. A specific AGC and analog-to-digital converter (ADC) design performing digital pulse blanking and dedicated to L5 receivers is also studied.

INTRODUCTION

The AGC implementation is a very important component in a GNSS receiver; it may be viewed as an adaptive variable gain amplifier whose main role is to minimize quantization losses. The AGC operation is tied directly to the analog-to-digital converter (ADC). For GNSS receivers in which the useful signal power is below that of the thermal noise floor, the AGC is driven by the ambient noise environment rather than the signal power. As a

result, AGC can be a valuable tool for assessing the operating environment of a GNSS receiver. Indeed, interfering signals will change the AGC gain as will be shown later in the paper.

The first part of the paper describes the classic model for the implementation of the AGC given the thermal noise environment. Next the behavior of this component in presence of different types of interference (continuous and pulsed) is assessed and simulated in order to highlight associated issues.

In the second part of the paper a theoretical study of an AGC dedicated to an L5 receiver is done. The careful design of the AGC component offers interesting possibilities to cope with expected interference in this frequency band. For example, the inclusion of a greater number of bits for quantization than will be processed by the correlator can offers significant advantages in case of pulsed interference, like that expected from the Distance Measuring Equipment (DME) the primary interference threat in the L5 band.

Finally, the third component of the paper presents hardware testing of an experimental dual frequency L1/L5 front-end design composed of 2 channels, one for each frequency. The focus of the design has been on the AGC and its ability to characterize the operational environments. This hardware has been tested in the lab with injected interference but also in actual environment so as to validate the theoretical study and assess its performance in real conditions.

AGC: ROLES AND MODES OF OPERATION

As shown in Figure 1, modern GNSS receivers are composed of an analog front-end component and a digital part that involves code and carrier tracking processes.

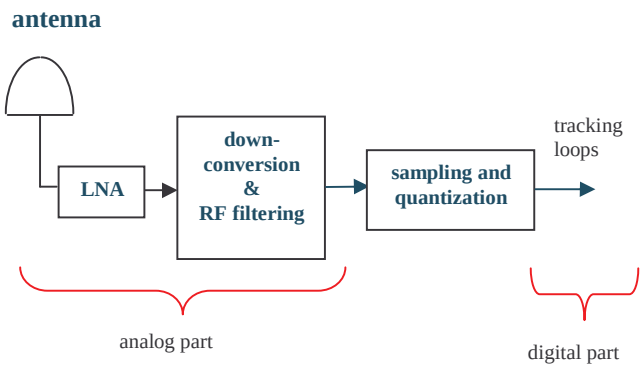

Figure 1 *Generic GNSS receiver diagram*

The "bridge" between these two components is the sampling and quantization of the analog signal. In the absence of any perturbation, such as interference or multipath, the incoming signal is the sum of useful GNSS signals and white Gaussian thermal noise. Different quantization laws may be adopted. The most prevalent ones are uniform although nonuniform techniques have been proposed, for example, to mitigate Continuous Wave (CW) interference in [Amoroso, 1983]. Quantization laws may be non-centered so that there is no zero level or centered. Figure 2 presents a uniform 2-bit non-centered law where the output signal takes value in the following bins: -3,-1, +1 or +3. The input sampled signal X corresponds to the x-axis while the output quantized signal X_Q is represented on the y-axis. L is called the maximum quantization threshold and Δ is the quantization interval.

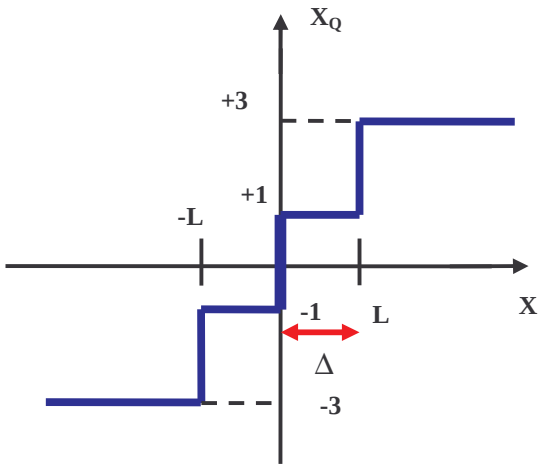

Figure 2 *2-bit non-centered and uniform quantization law*

Implementation losses in a GNSS receiver depend on the sampling rate, the quantization process and the precorrelation bandwidth, [Van Dierendonck, 1996]. All these parameters are related and have a combined effect. The associated loss may be expressed as the Signal-to-Noise ratio (SNR) degradation at the correlator output. For example, the established value for a 1-bit (hard limiter) quantization loss is 1.96 dB but this value is only true for infinite bandwidth and an infinite sampling frequency otherwise it is larger [Chang, 1982]. It can be shown that this degradation may be expressed as a function of the ratio of the maximum quantization threshold L to the input noise standard deviation σ. Surprisingly this expression does not depend on the signals themselves as they are negligible, below the noise floor, at this point in the receiver.

In presence of Gaussian thermal noise only, neglecting the precorrelation filtering and the limited sampling frequency, quantization losses are presented in Figure 3

and minimum degradations are summarized in Table 1 when using various bits widths for quantization.

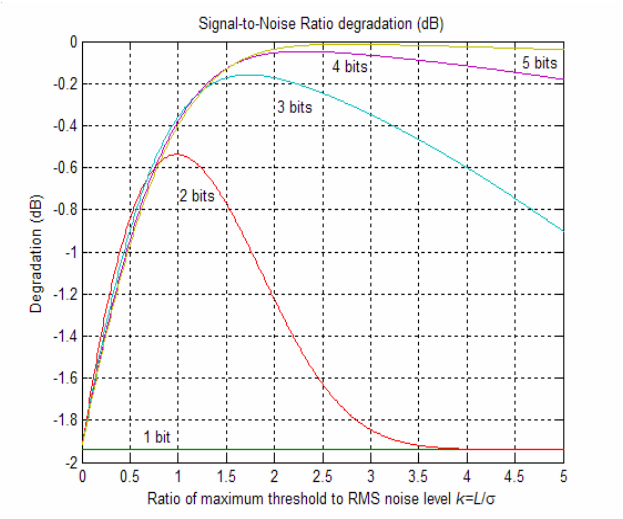

Figure 3 SNR degradation at correlator output due to quantization. Precorrelation filtering and finite sampling frequency effects are neglected

	1 bit	2 bits	3 bits	4 bits	5 bits
Optimal k	----	0.9860	1.7310	2.2910	2.2910
Minimum degradation (dB)	1.96	0.5369	0.1589	0.0138	0.0138

Table 1 Minimum SNR degradation due to quantization and associated optimal ratio. Precorrelation filtering and finite sampling frequency effects are neglected

As it is clear from the table, there is an optimal ratio k that minimizes quantization losses. Now it is possible to introduce the primary role of the AGC: it ensures that the optimal ratio is utilized. Another function of the AGC is to increase the dynamic range. For example, if an interferer appears it can cause saturation in the quantizer and even completely capture the process. By decreasing its gain, the AGC limits signal saturation. An important related consideration is the larger the number of bits, the less sensitive the SNR degradation to the AGC gain setting.

Assume quantization law is fixed as well as the maximum quantization threshold L. Thus AGC will be responsible to ensure that the Gaussian noise standard deviation takes the optimal value. Thus it is an adaptive system implemented as a feedback loop. It is typically located right before the Analog-to-Digital converter (ADC).

Different implementations of the AGC may be considered. The first type measures the analog signal itself to estimate the noise standard deviation and adjust the power of a amplification stage. Such an implementation is the most common and operates completely in the analog domain. However, as will be explained in a later section, such a design it is not very convenient if blanking is to be implemented. Thus only parts of the signal where known pulsed interference is absent should be considered to drive the AGC gain. Then, there is a digital implementation that uses ADC output samples to form metrics steering the AGC gain. Two different methods may be used: the conservation of the ADC bins Gaussian shape and the mapping of the ADC output signal power to the ADC input signal power.

It is known that in the absence of interference, the thermal Gaussian noise is the prevalent signal so that the observable distribution on ADC bins will be of a Gaussian shape. With the optimal ratio known, then the resulting optimal distribution of the ADC bins is determine. If this distribution is obtained then the SNR degradation is minimized. For a 2-bit uniform and non-centered quantization, the optimal distribution is shown in Figure 4.

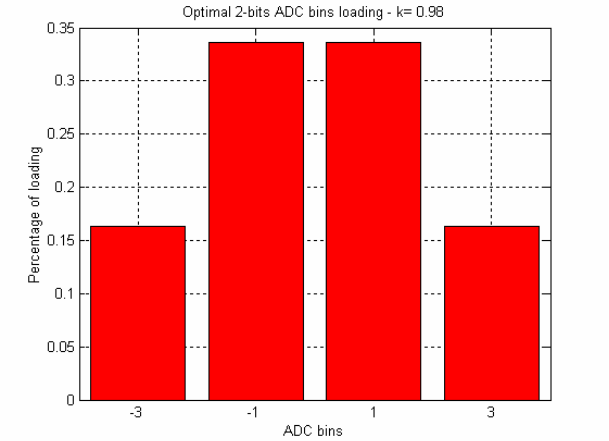

Figure 4 Optimal 2-bit non-centered and uniform quantization bins loading

Optimal loading for each bin from the left to the right is

16.35 % 33.65 % 33.65 % 16.35 %

A second way to control the AGC gain is to map the ADC output signal power to the ADC input signal power. Then using a look-up table, the receiver may estimate the input noise standard deviation by estimating quantized signal power.

To illustrate the behavior of the AGC gain, the next plot shows the Novatel OEM4 AGC gain change as a function of the input signal power increase. This test was done using a noise generator and increasing noise power during

the test. The variable noise source was coupled with the true L1 signal from an antenna.

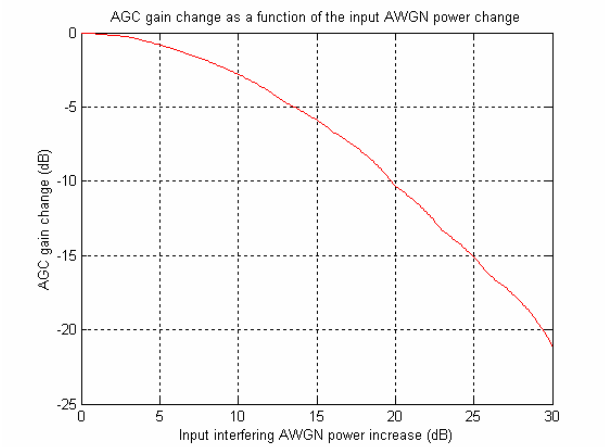

Figure 5 AGC gain change as a function of the input interfering AWGN power increase

The AWGN power increase is detected by the AGC and the receiver decreases its internal gain to conserve the optimal input signal standard deviation. The detection of potential interference is clearly possible by looking at the AGC gain variation with respect to the nominal case.

In the presence of constant power CW interference the SNR degradation at correlator output is described in [Van Dierendonck, 1996]. If the CW has a frequency offset with respect to the GNSS signal frequency larger than the predetection integration time or in case of large enough frequency modulation (FM) interference, degradation may be expressed as a function of the quantization interval. Figure 6 shows the SNR degradation, using 3 bits, at correlator output, in presence of a CW for various Jammer-to-Noise (J/S) ratios.

The issue is that if the receiver is not specifically designed to detect and cope with this kind of interference, it will adapt its AGC gain as if there is only thermal Gaussian noise present. In this case the adaptation is not optimal. The next plot in Figure 7 shows the SNR degradation in presence of a CW or FM in different configurations. The first corresponds to the absence of any AGC/ADC, known as the linear case. The second one is in the case of the optimal gain adaptation according to previous plot and the last one to the "blind" adaptation where only the presence of Gaussian thermal noise is assumed.

Thus, for large J/N ratios, the difference of degradation between the optimal and the classic adaptation may be large. For example, the result is about 10 dB for J/N=20 dB. Thus a receiver that is intended to mitigate CW simply using the AGC should adaptively change its quantizer interval. More complicated solutions, such as spectral excision of the CW at the ADC output, are also possible.

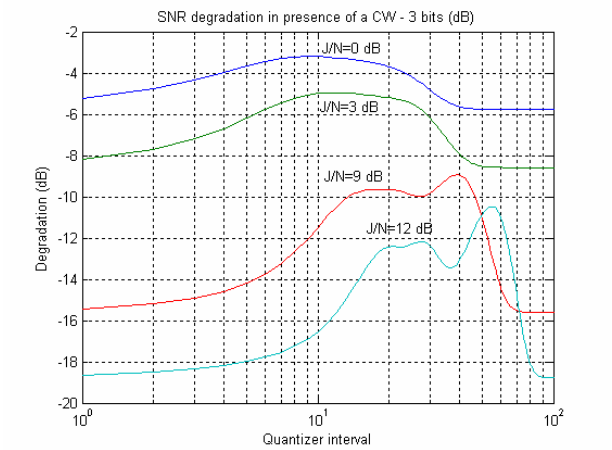

Figure 6 SNR degradation (3 bits) at correlator output in presence of a CW with large enough frequency offset with respect to the useful signal carrier frequency

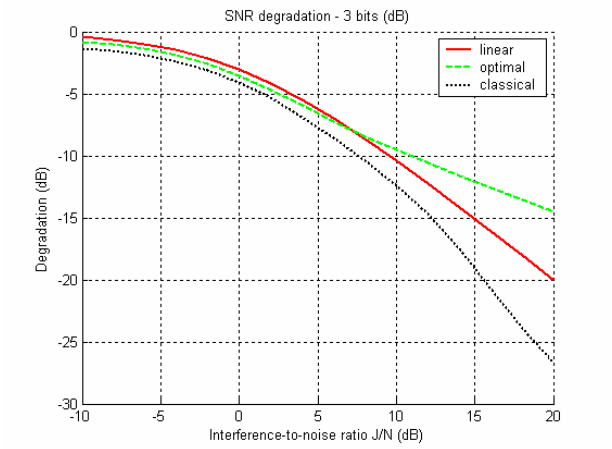

Figure 7 SNR degradation at correlator output in presence of a CW with large enough frequency offset with respect to the useful signal carrier frequency or FM. Different adaptation techniques are considered.

This section has presented classical results on Automatic Gain Control systems. The following section studies an AGC implementation dedicated to GNSS receivers to be used in the L5 band.

L5-SPECIFIC AGC/ADC IMPLEMENTATION

The expected GNSS L5 band interference environment is presented in [Hegarty, 1996]. It is documented that systems of significant infrastructure already exist in the L5

frequency band, with the main threat being the pulsed DME/TACAN signals. The initial proposal on how to cope with these signals was to implement pulse detection and blanking circuitry. This circuitry was first proposed using analog technology as explained in [Hegarty, 2000] but a digital solution was later proposed [Grabowsy, 2002]. This method is much simpler because no pulse detector circuit is required to identify the beginning and end of each pulse. Further, the implementation does not need memory to track samples that are part of a pulse. Samples are zeroed on a sample-by-sample basis as explained in the following paragraph. Even if there are some disadvantages, this method is likely to be one selected in future GNSS receivers as a result of the simplicity of the design.

As proposed in [Grabowsy, 2002], digital pulse blanking is implemented using an ADC having more bits than required in the digital tracking loops. In this published work, 8 bits were used to quantize the signal but the signal was eventually represented using only 3 of those 8 bits for further digital processing. The additional available bits were used to implement digital blanking.

The principle of the digital pulse blanking is simple. It relies on the fact that pulses are short, about 3 µs, and have very large amplitude as compared to the noise level. Each sample is quantized over the all available bins and its quantized value is compared to a threshold. If the value is above that threshold then the sample is set to zero as a pulse is declared to be present. The next plot, Figure 8, shows a possible bins loading repartition over 8 bits, the blanking threshold set on quantized signal amplitude and the associated blanking zones. Output values are between -255 and +255 with a step of 2 to ensure a non-centered uniform quantization law.

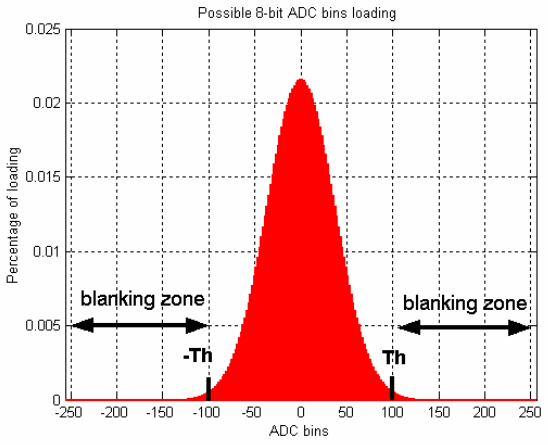

Figure 8 *Possible 8-bit bins loading in presence of thermal Gaussian noise only and the blanking thresholds*

The threshold Th is chosen as a compromise between the ability to detect pulses and C/N_0 degradation in the absence of pulses. It is important to recognize that depending on the noise standard deviation and the value of the threshold, there is a certain probability that valid samples are above the threshold so a portion of the useful signal will be blanked. Thermal noise is also lost but signal lost dominates. The SNR degradation is indicated, in this case, in [Grabowsky, 2002]. Obviously, the AGC gain setting should not take into account blanked samples because nominal operation of this system is in presence of thermal Gaussian noise only. Samples prior to digital pulse blanking may contain pulses and samples right after blanking include zeroes. The AGC gain setting would be respectively too low or too high.

Design of an AGC/ADC using more bits than required is a straight forward extension when compared with the classic design. Assume that bit_{init} bits (for instance 2) are initially used in digital tracking loops but a bit_{total}-bit (for instance 5 bits) ADC is available. From the first part of this paper, there is an optimal ratio $k_{opt} = \frac{L}{\sigma}$ that minimizes SNR degradation at correlator output. Assume parameter L is constant so there is an optimal incoming noise standard deviation σ_{opt}. The maximum quantization threshold is $L = \left(2^{bit_{init}-1} - 1\right)\Delta$ where the quantization interval is Δ. The partition that represents the limits between quantization intervals is $P = -L : \Delta : L$. Additional bits (bit_{total} - bit_{init}) may be used either to increase the resolution or increase the dynamic range. Assume bit_{res} additional bits are dedicated to increase the resolution then the new quantization interval is $\Delta_{new} = \frac{\Delta}{2^{bit_{res}}}$. Numbers of bits must, of course, comply with this relationship

$$bit_{init} + bit_{res} \le bit_{total}$$

where bit_{total} is the total number of available bits.
The new maximum quantization level is $L_{new} = \left(2^{bit_{total}-1} - 1\right)\Delta_{new}$ and the new partition is $P_{new} = -L_{new} : \Delta_{new} : L_{new}$. So as to obtain samples on bit_{init} bits, quantized samples on bit_{total} must be grouped according to the initial partition P.

The next plot, Figure 9, shows the ADC bins loading if 2 bits are used in digital tracking loops (optimal

ratio $k = 0.98$) but that 5 bits are available in total. Quantized values are between -31 and +31, by steps of 2, to ensure a uniform and non-centered quantization. Subplots correspond, respectively, to the absence of additional bits, 1 and 2 additional bits to increase resolution.

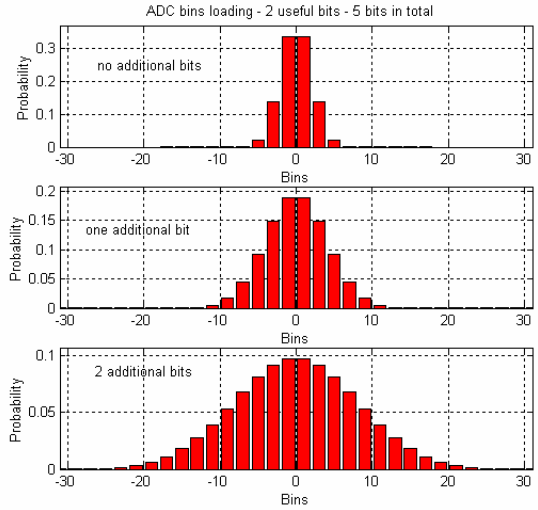

Figure 9 *ADC bins loading for 2 useful bits but 5 bits in total with several additional bits (0, 1 and 2) to increase resolution*

The maximum quantization threshold remains the same so that the feedback loop parameters are the same as those used in a 2-bit only case.

Additional bits may also be used to increase the dynamic range of the AGC. Assume the nominal bin distribution is chosen to be narrow over the full range as shown on the first subplot of previous figure. Then if a strong interference, such as a CW, appears the AGC gain will decrease to ensure the optimal ratio k. However the variable analog gain has a limited range such that the AGC gain cannot decrease below a certain fixed value. It may imply saturation in traditional AGC/ADC implementations. Now using more bits, bins distribution may spread out over the full range of bins preventing quantization from saturation. The global gain is then larger. Of course it means that the ADC must also be adaptive and the blanking threshold will not be constant. The dynamic range of the ADC using previous methodology is

$$2^{bit_{total}-1}.\Delta_{new} = 2^{bit_{total}-1}.\frac{\Delta}{2^{bit_{res}}} = 2^{(bit_{total}-bit_{res})-1}.\Delta$$

Clearly, dynamic range decreases as the selected resolution is large. Figure 10 illustrates the variation of the ADC dynamic range as a function of the additional bits used to increase ADC resolution. Table 2 summarizes these results. Again 2 bits are initially used in tracking loops and 5 bits are available in total. For this illustration, the initial (no additional bits) quantizer interval is set to 1 volt.

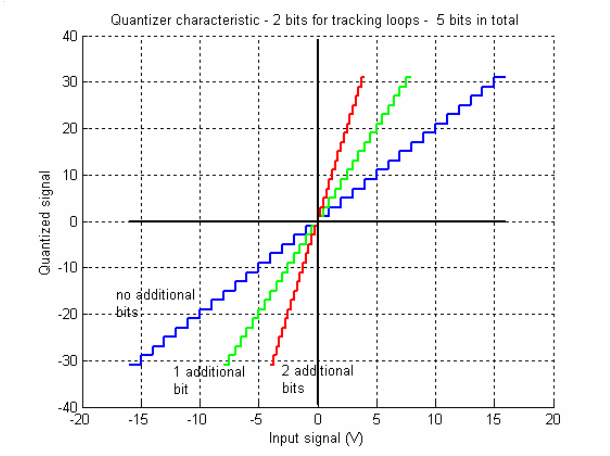

Figure 10 *Quantizer characteristic for 5 bits in total (2 bits initially) and with various additional bits for increased resolution*

number of additional resolution bits	0	1	2
dynamic range (V)	32	16	8

Table 2 *Dynamic range for O, 1 or 2 additional bits dedicated to resolution increase.*

As explained previously, available supplementary bins may be used to better represent the thermal noise Gaussian distribution through increased resolution. This additional resolution could bring higher interference detection performance. Recall that the ADC bins distribution is maintained constant, in the absence of any perturbation, as a result of the AGC gain adaptation. If an interference source is introduced, AGC gain decreases to try to maintain the Gaussian shape. Thus, even in presence of interference, the ADC distribution may seem to be nominal. However if the resolution is increased, the ADC distribution may clearly represent the distribution of the incoming signal. This distribution was previously hidden because of the low resolution. Indeed, the incoming signal distribution shape is unchanged by the AGC that only applies a gain. Thus it is possible to implement a test on ADC bins distribution changes to detect interference. A straightforward approach is to use the Chi-Square test to decide if two sets of data are consistent. The nominal distribution may be stored during an initialization phase when the receiver is turned on, assuming of course that no interference is present. Denote $n_{nom}(i)$ and $n_{current}(i)$ as the number of samples in the nominal case and in the

current situation for the i^{th} bin, respectively. Then the Chi-Square T is defined as

$$T = \sum_i \frac{(n_{current}(i) - n_{nom}(i))^2}{n_{current}(i) + n_{nom}(i)}$$

where the sum is defined over all bins. A large value of T indicates that the null hypothesis, the $n_{current}$'s and $n_{nominal}$'s are drawn from the same distribution, is rather unlikely. If the number of bins is large then the chi-square probability function is a good approximation to the distribution of T in the case of the null hypothesis. If data is collected in such a way that the sum of n_{nom}'s is the equal to the sum of $n_{current}$'s then the degrees of freedom is equal to the number of bins minus one. Then a significance level α is chosen, it is associated value S so that $\Pr ob(\chi^2 > S) = \alpha$. If the test T is larger than S then the null hypothesis is rejected and interfering signals are likely present. The significance level may be interpreted as the false alarm probability of the test. The next plot illustrates the use of a chi-square test to detect interference. A CW was generated at L1 and coupled with real GPS L1 signals. The resulting signal was provided to a Novatel OEM4 receiver. During the test, interference power was gradually increased until receiver loss lock then it was decreased. Significance level is chosen to be 0.05.

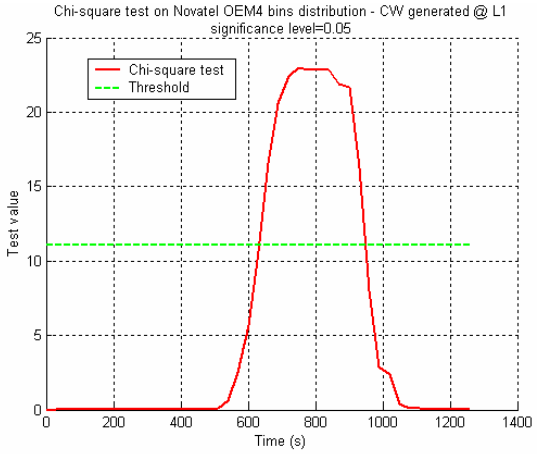

Figure 11 Chi-square test value during a test where a CW @ L1 was coupled with real signals and provided to a Novatel OEM4 receiver

Clearly this test enables to detect interference even if a few bits are used (e.g., 2.5 for this receiver). However the interference is likely to be detected earlier if more bits are used.

Thus the designer has the choice of the repartition of the total number of bits. It is a trade-off between ADC resolution and AGC/ADC total dynamic range. The repartition should not be too spread significantly so as to increase the maximum achievable dynamic range. If the Chi-square test is implemented to detect interference, more bins to represent the distribution are preferable even if very good results are achieved using a few bits. An increased resolution may also allow interference identification by performing tests, for instance maximum likelihood estimation, on the ADC distribution.

L1/L5 BAND ENVIRONMENT MONITOR

An L1/L5 environmental monitor was constructed to enable monitoring of the radio frequency environment of the L1 and L5 bands. Although there is no current GNSS signal on L5, the hardware developed will suffice once such signals are available as the received power levels are expected to be at approximately the same levels as the thermal noise floor.

The constructed hardware is shown in block diagram format in Figure 12 and a photograph of the equipment is shown in Figure 13.

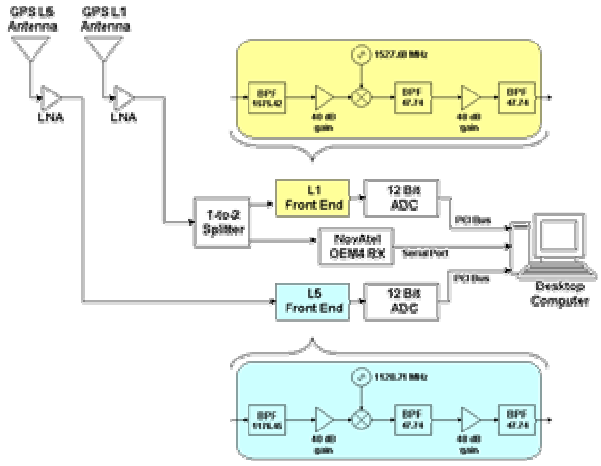

Figure 12 Hardware setup diagram

Both L1 and L5 frequency bands are downconverted, filtered, and amplified to exercise a majority of a 12-bit ADC. There are two distinct channels for L1 and L5.

On the left hand side of the photo in Figure 13 there are signals generators and the Novatel OEM 4 receiver. The front-end is the middle and the computer on the right. The computer is used to store tests results.

THREE DAY DATA CHARACTERIZATION

A nominal test over three consecutive days was conducted at Stanford University. The equipment continually gathered 40ms "snapshots" of raw IF data approximately every minute. The objective was to characterize L1 and L5 bands in nominal conditions at Stanford University

.

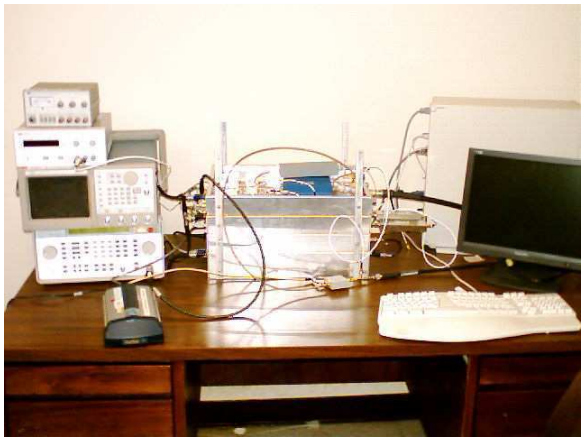

Figure 13 *Hardware setup photo*

In parallel with the operation of the L1/L2 environmental monitor a Novatel OEM4 receiver used. The output of the GPS antenna, a Novatel Pinwheel, was split into two paths: the first for the L1 environment monitor and the second for the OEM4 receiver. Various messages were logged from the receiver with the focus on the AGC message as to directly compare the results of both implementations. It is important to recognize that the AGC message from traditional GPS receiver can be monitored to determine if there is a relative change in the operating environment, such as the introduction of an interference source, however there is little that can be determined about the nature of the interference source. Characterization is the function of the constructed environmental monitor.

In Figure 14 is an example of raw data measurements on both L1 and L5 bands. For each band, there are a power spectral density plot, the ADC bins distribution and a temporal plot of the quantized signal. Approximately the same amplification levels are used in the L1 and L5 channels of the environmental monitor, yet the results look significantly different.

The L1 band looks relatively interference free with the traditional Gaussian distribution of the samples and results filter characteristics in the frequency domain. In contrast, there are clearly pulsed signals in the L5 band. According to the PSD plot, central frequency of this interference is offset from L5 by about -3 MHz. After further investigation, it was discovered that the DME ground station of Woodside, CA (about 6 miles from Stanford) transmits its signal at 1173 MHz. The observed signal on raw data corresponds undoubtedly to this DME signal, next plot, Figure 15, confirms that. It is a close-up of a portion of previous L5 raw measurement.

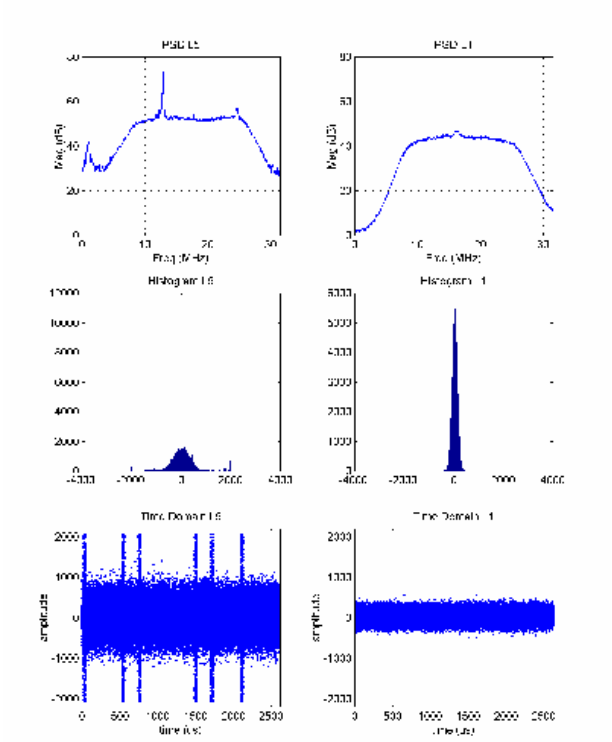

Figure 14 *L1L5 raw data PSD, histogram and temporal plots*

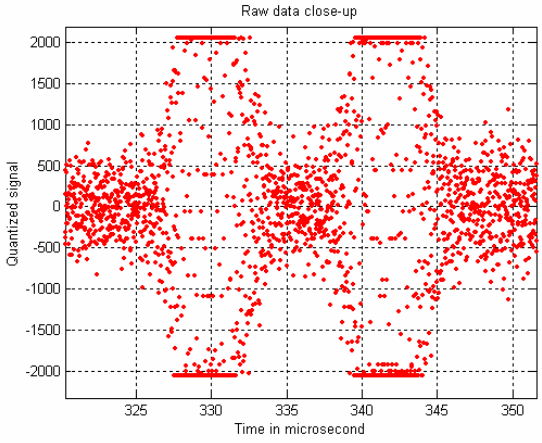

Figure 15 *L5 raw data close-up*

The inter-pulse interval is about 12 μs and the half amplitude width is about 3.5 μs as the X-mode of DME signals.

The signal was consistently visible for the duration of the testing in the L5 band.

Within the L1 band, the data from the environmental monitor almost exclusively appeared as white noise with no interference characteristics. However, on less than 0.5% of the data sets, at random times, what appears to be very short pulsed interference signals were observed within the L1 band as depicted in Figure 16.

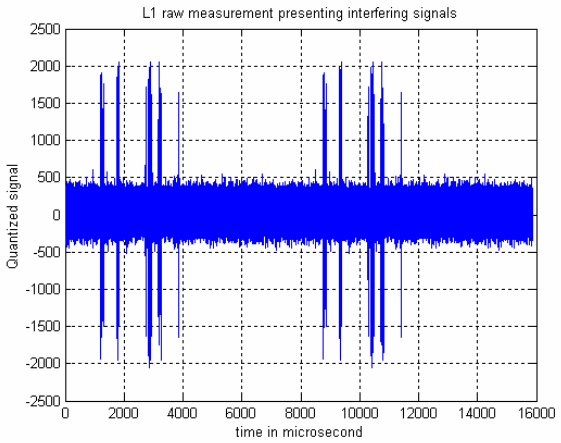

Figure 16 *L1 raw measurement presenting interfering signals*

As a result of the random nature and infrequent appearance, it was not possible to determine what their origin was. Further monitoring/characterization can be combined with direction finding to aid in locating the source of such interference.

In parallel with the environment monitor data collection, the AGC message from the Novatel receiver was logged and the results from two days of data are plotted in figure 17.

.

Upon careful observation, the AGC gain varies periodically by about 1 dB during the test. This result can also be deduced from the data collected by the environmental monitor, yet illustrates the sensitivity of the AGC message of the OEM4 receiver.

Upon first inspection, it appears that their there is fluctuation the noise floor of the receiver that is periodic with time. However, later investigation revealed that the AGC gain is higher during hotter periods of the day (around 16/17). This is clearly shown when the ambient temperature for antenna is monitored, as shown in Figure 18.

The first assumption was that thermal noise increases when temperature is higher with the presence of the sun, a thermal radiator, in the sky. However, if that were true, the gain should be lower. After some further investigation it was determined that the basis for the change in the AGC is the decrease of the nominal gain of amplifier(s) present in the antenna. As the temperature increases the efficiency of that amplifier decreases, with each stage affecting the overall contribution.

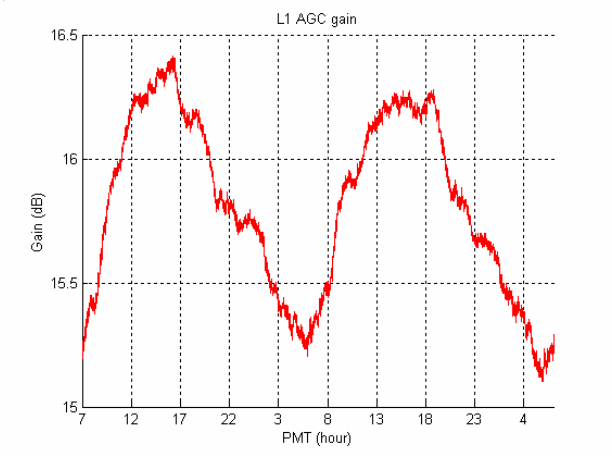

Figure 17 *L1 AGC gain over 2 days*

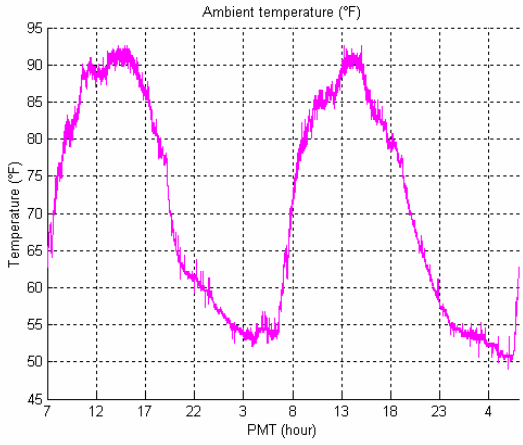

Figure 18 *Ambient temperature over 2 days*

Clearly there is a correlation between the nominal noise floor (observed via the AGC gain) and ambient temperature (or its impact on the amplifier). Such effects need to be quantified or better attention needs to be given the overall design to allow AGC to be used as an interference detection source. However, the change observed in this case is relatively minor and thus even if it was completely neglected, the current implementation would still be quite valuable for interference detection.

DME SIGNAL INECTION

An analog DME-like signal was constructed using an arbitrary waveform generator (AWG). The signal is periodical with a period of 305 microsecond so there are about 3300 pulse pairs per second. A real DME pulse is well represented by a Gaussian shape signal and was so simulated according to the following formula [Monnerat, 2001]

$$s_{DME}(t) = e^{\frac{-\alpha t^2}{2}} + e^{\frac{-\alpha(t-\Delta t)^2}{2}}$$

where

- α =4.5e11 s^{-2}
- Δt =12e-6

Each pulse has a 3.5 μs half-amplitude width and there is a 12 μs inter-pulse interval. The next plot, Figure 19, shows such the resulting digital waveform which was converted to an analog signal using the AWG.

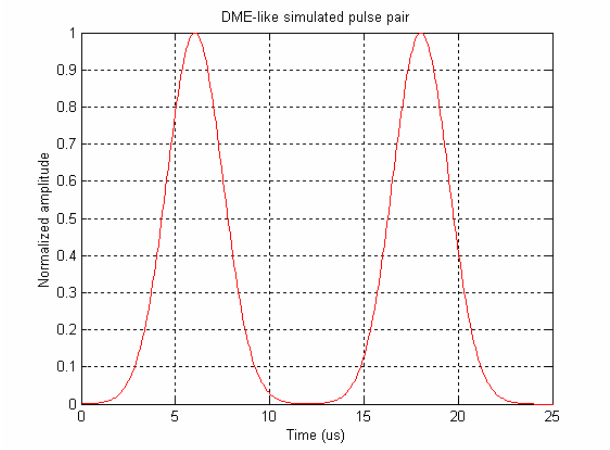

Figure 19 *Simulated DME pulse pair*

This analog signal was mixed with a carrier frequency of 1573.0 MHz, offset by 2.42 MHz from the GPS center frequency, and injected with varying power levels using the configuration depicted in Figure 20. As shown, the interference signal is combined with "live" GPS data from the antenna so that impact of the interference can be quantified on the processing.

Shown in Figure 21 is result in the time domain of the injected signal on the environmental monitor. The difference between the nominal environment and that of the interference injection scenario is obvious. It is also clear that DME-like pulses occur at a much higher rate than that observed in the L5 data. However, this experiment was constructed to emulate a DME operating at close to full capacity.

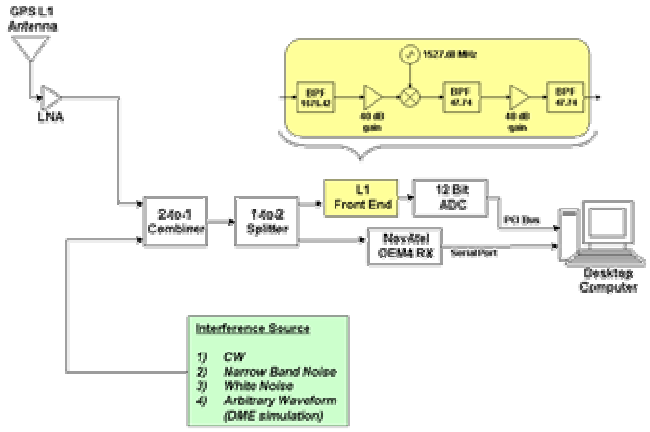

Figure 20 DME/Interference Injection Experiment

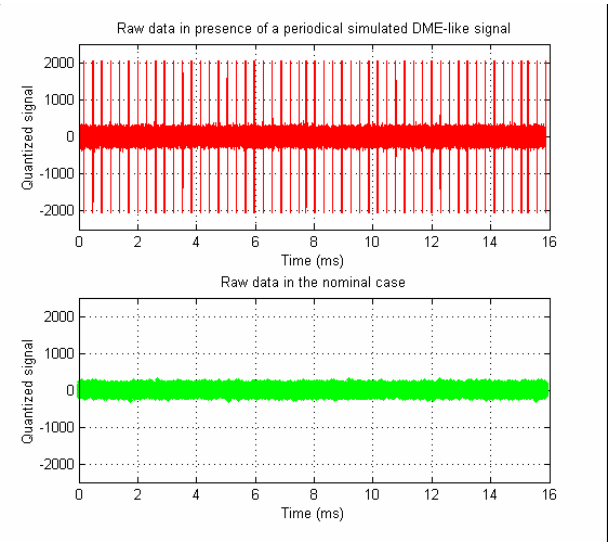

Figure 21 *Temporal raw measurement in presence of the periodical simulated DME-like signal and in the nominal case.*

The presence of the DMA-like pulses is also clear in the frequency spectrum plot of the data collected by the environmental monitor. Note that this spectrum looks quite similar to that observed by for the L5 band environmental monitor, a goal of this experiment. Also note that the spike in the spectrum appears above the nominal IF component of 47.74 MHz rather than below, where it might be expected with the carrier at 1573 MHz. This is merely a result of the aliasing of the passband in the sampling of the signals.

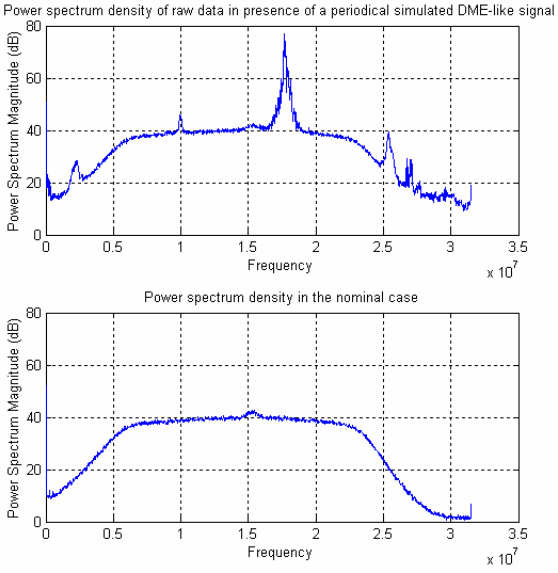

Figure 22 *PSD of the periodical simulated DME-like signal and in the nominal case*

What is of particular interest is the impact such a signal has on the traditional GPS receiver as the result can foreshadow what might be expected for the GPS signal processing in the L5. Of course, the L5 signal structure is significantly different than that for L1 (wider band, in particular) and it is likely that problematic DME signals within the L5 band will attempted to be relocated and also receiver designs for L5 will incorporate some type of receiver blanking to minimize the pulsed impact.

The first plot of the results from the Novatel is shown in Figure 23. This plot shows the L1 AGC gain variation as a function of the input interfering DME-like signal power increase.

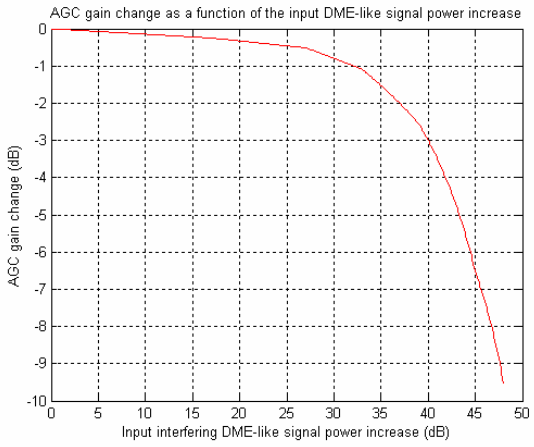

Figure 23 *AGC gain change as a function of the input DME-like signal power increase*

This plot shows the change in the AGC of the GPS receiver as a function of the input power of the DME-like signal. As expected for pulsed signals, there is not a one-to-one change in that relationship.

The impact of the simulated DME-like signal on the real received L1 signals is well observable on the C/N_0 reported by the Novatel OEM receiver. Next plot shows this information as reported by the receiver for 3 different SVs being tracked during the time of signal injection.

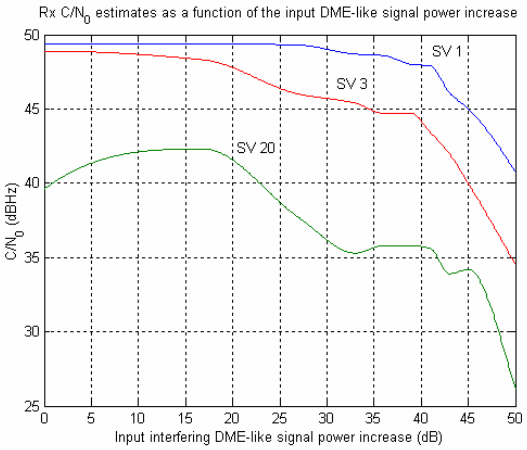

Figure 24 *Novatel OEM4 C/N_0 estimates variation as a function of the DME-like signal power increase for 3 SV's*

As the simulated interference power increases, estimated C/N_0 decreases. Thus this starts to illustrate the potential impact of having a DME signal within the GPS band. Further efforts will investigate mitigation techniques described earlier in this paper.

CONCLUSIONS

The AGC system has been shown to be an accurate indicator of noise environment of the receiver. Its gain varies with respect to the present interference power and so is a valuable tool to detect them. Moreover the ADC bins distribution may be also used to detect interference by using a simple Chi-square test detecting distribution changes.

The developed hardware also turned out to be a very efficient tool to assess the interference in L1 and L5 bands. It is transportable and so may be easily used at different locations.

Acknowledgments

The authors would like to acknowledge the assistance of Mike Koenig for antenna and ambient temperature measurements.

References

[Van Dierendonck, 1996] A.J. Van Dierendonck, "GPS receivers", Global Positioning System: Theory and Application, B.Parkinson and J.J Spilker, JR., Ed ., Washington, D.C.: AIAA, Inc., 1996

[Chang, 1982] H.Chang, "Presmapling, Filtering, Sampling and Quantization Effects on the Digital Matched Filter Performance", *Proceedings of the International Telemetering Conference, 1982, pp. 889-915*

[Hegarty, 1996], Hegarty, C., T. Kim, S. Ericson, P. Reddan, T. Morrissey, and A.J. Van Dierendonck, "Methodology for Determining Compatibility of GPS L5 with Existing Systems and Preliminary Results," *Proceeding of The Institute of Navigation Annual Meeting, Cambridge, MA, June 1999*.

[Hegarty, 2000] Hegary, C., A.J. Van Dierendonck, D. Bobyn, M. Tran, T. Kim, J. Grabowski, "Suppressing of Pulsed Interference through Blanking." *Proceedings of the IAIN World Congress, San Diego, CA, June 2000*.

[Grabowsky, 2002] Grabowski, J, Hegarty, C, "Characterization of L5 Receiver Performance Using Digital Pulse blanking", *Proceeding of The Institute of Navigation GPS Meeting, Portland, OR, September 2002*.

[Monnerat, 2001] Monnerat, M, Lobert, B, Journo, S, Bourga, C, "Innovative GNSS2 navigation Signal", *Proceeding of The Institute of Navigation GPS Meeting, 2001*

[Amoroso, 1983] F.Amoroso, "Adaptative A/D Converter to Suppress CW interference in DSPN Sread-Spectrum Communications", *IEEE Transactions on communications, VOL.COM-31, NO.10, OCTOBER 1983*